Combined Steering and Direct Tilt Control for the Enhancement of Narrow Tilting Vehicle Stability

James W. Robertson, Jos Darling, Andrew R. Plummer
Department of Mechanical Engineering, University of Bath, Bath, United Kingdom.

Corresponding Author: James Robertson, Department of Mechanical Engineering, University of Bath, Bath, Somerset, BA2 7AY, UK. Email: j.w.robertson@bath.ac.uk. Tel: 01225 384019.

Abstract:

Narrow Tilting Vehicles offer an opportunity to reduce both traffic congestion and carbon emissions by having a small road footprint, low weight, and a small frontal area. Their narrow track requires that they tilt into corners to maintain stability; this may be achieved by means of an automated tilt control system. Automated tilt control systems can be classed as Steering Tilt Control (STC) in which active control of the front wheel steer angle is used to maintain stability, Direct Tilt Control (DTC) in which some form of actuator is used to exert a moment between the tilting part(s) of the vehicle and non-tilting part(s), or a combination of the two (SDTC). Combined Steering Direct Tilt Control systems have the potential to offer improved performance as, unlike STC systems, they are effective at low speeds whilst offering superior transient roll stability to DTC systems. This paper details the implementation of a SDTC system on a prototype narrow tilting vehicle and presents experimental results which demonstrate a 36% reduction is load transfer from the inside wheel to the outside wheel during a ramp steer manoeuvre when compared to a DTC system.

Keywords: Narrow Tilting Vehicle, Steering Direct Tilt Control, Active Steering

1. INTRODUCTION

Narrow Tilting Vehicles (NTVs) offer the potential to alleviate two pressing urban transportation problems; traffic congestion and carbon emissions, whilst retaining the degree of personal mobility that modern society takes for granted. Compact dimensions, particularly the narrow body style, enable a greater number of vehicles to occupy a given road space thus reducing traffic congestion. Carbon emissions are reduced as a result of low vehicle mass and decreased aerodynamic drag forces associated with the small frontal area. NTVs also offer significant safety advantages over alternatives such as motorcycles and scooters [1]. Whilst NTVs have many potential benefits, their configuration presents some fundamental challenges; not least that their tall, narrow body styles make them vulnerable to overturning during vigorous manoeuvres.

In order to overcome the tendency to overturn, NTVs are equipped with a tilting mechanism that allows them to lean into bends in much the same way as a motorcycle [2]. NTVs can be classified in one of three broad categories; Passive Tilt Control, Steering Tilt Control (STC) and Direct Tilt Control (DTC). Passive Tilt Control describes vehicles in which the driver is solely responsible for maintaining the stability of the vehicle through steering inputs and shifts in body weight. This is the system employed by motorcycles and bicycles. It requires considerable skill from the operator, and an additional means of stabilisation at very low speeds or when stationary.

Vehicles equipped with STC relieve the driver of the task of maintaining stability by automatically making steering inputs that balance the vehicle at the desired tilt angle. In order for STC to function, the mechanical link between the driver's steering wheel and the steered wheel(s) must be broken and some form of active steering system introduced. Whilst STC systems work well at high speeds where modest front wheel steer angles generate large lateral accelerations, at low vehicle speeds, very large steering

inputs are required [3]. Thus, as is the case with passive tilt control, an additional stabilisation mechanism is required at very low speeds and when stationary.

As with STC, DTC relieves the driver from the responsibility of maintaining vehicle roll stability. DTC systems generate a tilting moment through the use of actuators linked to the suspension or non-tilting parts of the body rather than through use of the front wheel steer angle. Systems of this type have the considerable advantage that they are effective at low speeds (and whilst stationary) as the magnitude of the tilting moment is independent of vehicle speed. However, in highly transient conditions the tilting moments generated by DTC systems are significant; these moments cause variations in vertical load supported by the tyres and, if large enough, can lead to vehicle roll-over. In addition, the power consumption of DTC systems can be considerable [4].

Systems that combine both STC and DTC, i.e. systems which use both the front wheel steer angle and direct actuation to control the tilt angle may be referred to as Steering Direct Tilt Control (SDTC). Such systems aim to combine the transient stability and low power consumption associated with STC, with the low speed stability of DTC. Systems of this type have been proposed by a number of authors including Snell [5], Kidane *et al.* [6], So and Karnopp [7] and Berote *et al.* [8]. Whilst the effectiveness of SDTC control strategies has been demonstrated in simulation, there remains a lack of experimental verification of these results. Some experimental verification has been provided by Kidane *et al* [6,9] but the manoeuvres considered are relatively gentle ramp and sine wave inputs which occur over prolonged time periods and which generate lateral accelerations not exceeding 2.6m/s^2. Furuichi *et al*. [10] & [11] did provide some experimental verification of the performance of their SDTC system in a limited number of vigorous manoeuvres; however, the experimental conformation of vehicle stability was limited to confirming whether wheel-lift-off did or did not occur.

2. THE CLEVER VEHICLE

The ‘Compact Low Emission VEhicle for uRban transport’ (CLEVER) is a two seat narrow tilting vehicle developed using European Union funding by a number of industrial and academic partners. The original project brief was completed in 2006; the resulting vehicle featured a hydraulic Direct Tilt Control (DTC) system acting to tilt the cabin relative to a non-tilting rear module containing the engine and drive systems. A total of five CLEVER Vehicle prototypes were built; three were used in crash tests, one vehicle was fitted with bodywork and used for display purposes (Figure 1) while the final vehicle was retained by the University of Bath.

Figure 1: The CLEVER Vehicle complete with bodywork.

During testing of the prototype CLEVER Vehicle, it was found that the DTC system was un-able to guarantee vehicle roll stability under all circumstances, particularly during highly transient manoeuvres where the vehicle exhibited a tendency to lift an inside rear wheel during corner entry (Figure 2), often leading to capsize [12].

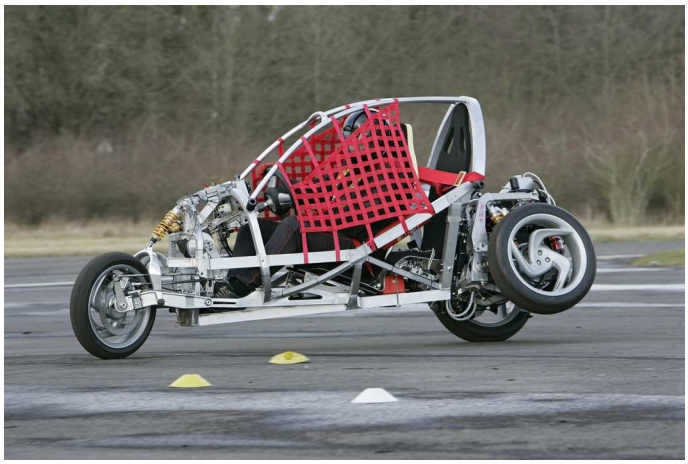

Figure 2: CLEVER Vehicle prototype demonstrating its lack of roll stability in transient conditions.

To further investigate the stability of the CLEVER Vehicle in transient conditions, a comprehensive multi-body simulation model of the CLEVER Vehicle was developed and verified in [8] & [13]. The simulation model was used to develop a SDTC strategy and subsequently derive a linearised model. The linearised model response was analysed in the frequency domain to demonstrate that the SDTC strategy led to a significant reduction in the load transfer across the operating range of the tilt control system. Analysis of results obtained using the non-linear model in the time domain showed that the SDTC system led to load transfer reductions of 70% and 43% respectively during figure-of-eight and step-steer input manoeuvres conducted at a forward speed of 8.3m/s [8].

This paper aims to provide experimental roll stability performance verification of the SDTC system proposed in [8] during severe, highly transient, manoeuvres with high lateral accelerations. These results will be compared to results obtained using the same vehicle in a DTC configuration and thus the stability enhancement provided by the SDTC strategy will be quantified.

Moment Reserve

Since only a proportion of the CLEVER Vehicle's mass can be tilted into the bend, and there are practical limitations on the extent to which the cabin can be 'over-tilted', it is not always possible to achieve a zero steady state roll moment when the vehicle is subjected to lateral accelerations. During transient conditions, the rear module may be subjected to an additional roll moment generated by the DTC actuators. If the combined roll moment is larger than the moment capacity of the rear module, wheel lift and possible capsize, will occur.

The concept of a 'moment reserve' was introduced by Berote [13] as a means of quantifying the maximum moment the DTC system could exert without causing wheel lift. The moment reserve can be calculated by considering the moments acting on the CLEVER Vehicle when in a steady state cornering condition, and subtracting this value from the total moment capacity.

The model shown in Figure 3 is used to derive equations for the moment reserve; it is simplified by assuming a rigid chassis with no suspension or tyre compliance, by constraining the yaw motion of the rear module and by ignoring pitch motions coupled to the tilt motion (and therefore variations in tilt bearing height (h_{tb}) and tilt axis inclination (ξ)). In addition, the mass of the rear module is assumed to be directly over the rear axle and the front wheel steer angle (δ_f) is assumed to remain zero.

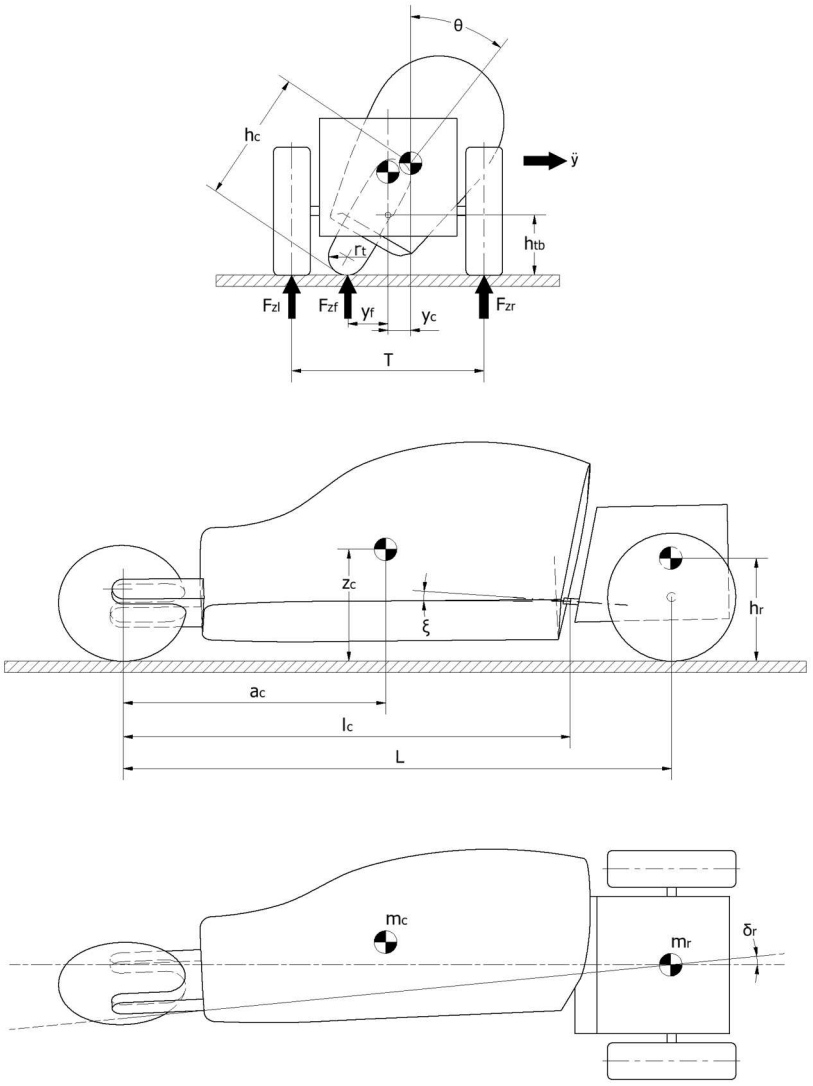

Figure 3: CLEVER Vehicle kinematic parameters with rear module constrained in yaw.

As a consequence of the raised and inclined tilt axis, with the rear module constrained in yaw, a lateral displacement of the front tyre contact patch occurs when the cabin tilts. In practice the displacement of the front tyre contact patch manifests itself as a rear wheel steer angle (δ_r); this has been designed into the CLEVER Vehicle to reduce oversteer and thus produce a neutral handling characteristic [12].

The lateral displacement of the cabin centre of gravity (y_c) and the lateral displacement of the front tyre contact patch (y_f) are given by:

$$y_c = \sin\theta\left[h_c - h_{tb} - \xi(l_c - a_c)\right] \quad \textbf{(2.1)}$$

$$y_f = \sin\theta\left[h_{tb} - r_t + \xi l_c\right] \quad \textbf{(2.2)}$$

The vertical height of the cabin centre of gravity also changes as a result of the tilting motion:

$$z_c = \cos\theta\left[h_c - \left(h_{tb}\frac{a_c}{l_c}\right)\right] + h_{tb}\frac{a_c}{l_c} \quad \textbf{(2.3)}$$

The tilt angle of the cabin (θ) is a function of the lateral acceleration ($\ddot{y}$) and an 'over-lean' factor of 1.2 (see 'Control Strategy' section):

$$\theta = 1.2 \times \left(\frac{\ddot{y}}{g}\right) \quad \textbf{(2.4)}$$

Taking moments about the centre of the rear track (on the ground plane) gives a roll moment of:

$$M = (m_c g y_c) + (F_{zf} y_f) - (m_c \ddot{y} z_c) - (m_r \ddot{y} h_r) \quad \textbf{(2.5)}$$

The total roll moment capacity (M_c) of the rear engine module is taken to be the maximum moment that can be applied to the rear engine module without a rear wheel lifting clear of the ground, (F_z>0). Assuming an even load distribution between the two rear wheels when stationary and with the cabin

upright, M_c can be expressed as a function of the rear tyre vertical loads (F_{zl} & F_{zr}) and the track width (T):

$$M_c = \pm(F_{zl} + F_{zr})\frac{T}{2} \quad \textbf{(2.6)}$$

The steady state moment reserve M_r in either direction is therefore given by:

$$M_r = [\pm(F_{zl} + F_{zr})\frac{T}{2}] + [(m_c g y_c) + (F_{zf} y_f) - (m_c \ddot{y} z_c) - (m_r \ddot{y} h_r)] \quad \textbf{(2.7)}$$

Table 1: Moment reserve parameter values

Symbol	Description	Unit	Value
a_c	Longitudinal position of cabin mass from front axle	m	1.158
F_{zf}	Vertical load supported by front wheel at rest	N	1242
F_{zl}	Vertical load supported by left rear wheel at rest with cabin upright	N	1400
F_{zr}	Vertical load supported by right rear wheel at rest with cabin upright	N	1400
g	Acceleration due to gravity	m/s^2	9.81
h_c	Height of cabin mass CG from ground plane in upright position	m	0.59
h_r	Height of rear module mass CG from ground plane	m	0.54
h_{tb}	Height of tilt bearing from ground plane	m	0.271
L	Wheelbase length	m	2.4
l_c	Longitudinal position of tilt bearing from front axle	m	1.953
m	Total vehicle mass (including driver)	kg	412
m_c	Cabin mass (including driver and un-sprung mass)	kg	250
m_r	Rear engine module mass (including un-sprung mass)	kg	162
r_t	Radius of tyre cross section	m	0.07
T	Track width	m	0.84
ξ	Tilt axis inclination from horizontal plane	rad	0.0873

The parameter values given in Table 1 are used to calculate the steady state moment reserve. Plotting the moment reserve against the lateral acceleration gives an indication of the maximum moment that the DTC actuators can apply without causing wheel lift off, Figure 4. The cabin reaches its maximum tilting angle of ±45° at a lateral acceleration of 6.41m/s^2 and the maximum possible lateral acceleration without capsize is 9.51 m/s^2. The data plotted in Figure 4 is likely to be an overestimate of the moment reserve as it excludes the influence of the rear module roll angle and tyre compliance (which if included would act to reduce the effective tilt angle). Since the tilt angle (θ) will not track the demand (θ_d) precisely, in transient conditions there is also likely to be a tilt angle error; this means the moment reserve will be lowered further.

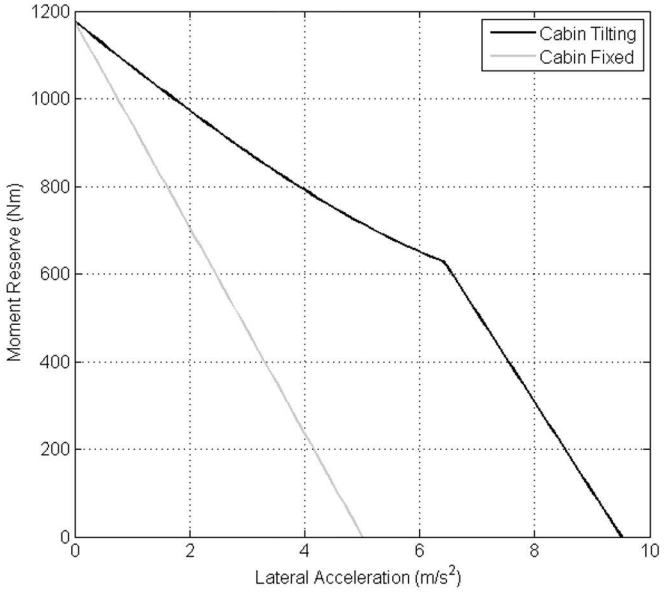

Figure 4: Steady state moment reserve shown with the cabin both tilting and fixed upright.

Whilst, according to Figure 4, the CLEVER vehicle can safely reach lateral accelerations approaching 1g in steady state, wheel lift-off has been observed from the prototype under transient conditions at lateral

accelerations of less than 4m/s^2. In highly transient situations large tilt angle errors are generated; these tilt angle errors act to both reduce the stabilising influence of the cabin mass (and therefore reduce the available moment reserve), and also to prompt the generation of tilting moments from the DTC actuators. Thanks to the simultaneous reduction in the moment reserve and the application of the tilting moment, the moment reserve may be exceeded and wheel lift can occur.

Although filtering of the tilt angle error (θ_e) is used in the controller to regulate the tilting response (see Control Strategy section), a strategy of further limiting the DTC actuator moment in transient situations is not considered viable; slowing the cabin tilt response would increase the tilt angle error, and in turn, lower the available moment reserve still further. Alternatively, controlling the front wheel steer angle with an active steering system could make two contributions to improving stability; firstly, the generation of lateral accelerations in response to a driver's steer inputs could be delayed giving time for the tilting action to occur before the moment reserve is depleted. Secondly, a momentary countersteering action could be generated creating a reverse lateral acceleration and generating a tilting moment that assists the DTC actuators.

3. IMPLEMENTATION OF A STEERING DIRECT TILT CONTROL STRATEGY

In order to facilitate Steering Direct Tilt Control of the CLEVER Vehicle it was necessary to supplement the existing DTC hardware with an active steering system. To this end, a hydraulic 'in-series' active steering system capable of altering the front wheel steer angle by 5.6º in either direction was fitted to the prototype. The term 'in-series' is used in this context to describe an active steering system that, rather than sever the driver's mechanical connection to the front wheel completely, contains a means of modifying that connection to influence the front wheel angle; see Figure 5. This type of system has the

advantage that, when the active steering system is idle, normal steering feel is retained and no artificial steering feedback need be created.

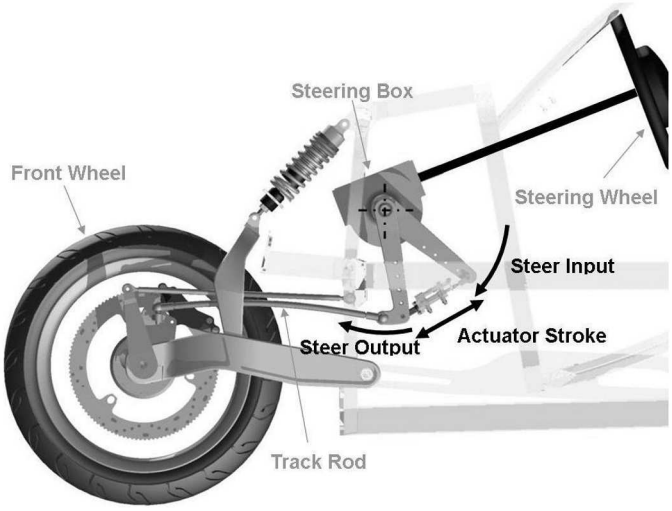

Figure 5: In-series active steering actuator installation.

Control Strategy

In [8] Berote *et al.* propose a SDTC strategy in which both DTC and STC systems work simultaneously to achieve a common tilt angle demand throughout the entire speed range of the CLEVER Vehicle. The controller used the driver's steer demand and the vehicle's speed to estimate the lateral acceleration, and hence the tilt angle required to stabilise the vehicle. A variable active steering gain changes the magnitude of the steer angle alterations in response to the vehicle's forward speed, with smaller alterations being generated at higher speeds. It is this strategy that forms the basis for the SDTC system implemented in this paper.

Using small angle approximations, assuming no tyre slip and ignoring both front wheel camber angle and rear wheel steering angle (δ_r), the cornering radius (r) is given by:

$$r = \frac{L}{\delta_d} \tag{3.1}$$

Where L is the vehicle wheelbase and δ_d is the driver's demand steer angle.

The lateral acceleration ($\ddot{y}$) is obtained from the cornering radius (r) and the vehicle's forward speed (U):

$$\ddot{y} = \frac{U^2}{r} \tag{3.2}$$

Using small angle approximations, the tilt angle (θ_d) required for balanced cornering is given by:

$$\theta_d = \frac{\ddot{y}}{g} \tag{3.3}$$

An additional empirically derived 'over-lean' factor of 1.2 is then applied to the equilibrium angle to compensate for the reduced effective tilt angle (arising from the rear module roll angle and the tilting kinematics) and the mass of the non-tilting rear module [14]. Note that the maximum magnitude of the over-lean factor is limited, too high and the driver may perceive a lateral acceleration away from the corner centre.

$$\theta_d = 1.2 \times \left(\frac{\ddot{y}}{g} \right) = 1.2 \times \left(\frac{U^2}{gL} \delta_d \right) \tag{3.4}$$

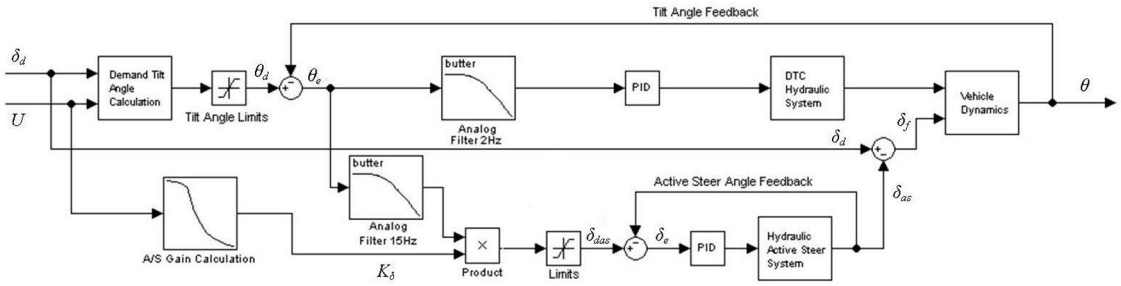

Figure 6: SDTC system block diagram.

The demand tilt angle (θ_d) and the instantaneous tilt angle (θ) are used in a closed loop negative feedback position control system, Figure 6. The tilt error signal (θ_e) is subjected to a 2Hz low pass filter, the frequency being chosen to remove unwanted noise and limit the transient DTC actuator torque [15]. A hydraulic proportional valve linked to a pair of single acting tilt actuators is used to generate the tilting moment whilst a linear position sensor mounted to one of the tilt actuators is used to provide the necessary position feedback signal.

The active steering controller generates an active steer demand angle (δ_{das}) that is a function of the tilt angle error (θ_e) multiplied by a non-linear speed dependent active steering gain (K_δ). Note that the tilt angle error used in the active steering controller is filtered at a higher frequency than the same signal in the DTC controller in order to facilitate a faster response. The active steer demand angle is used in a second negative feedback position control loop with a Linear Variable Differential Transformer (LVDT) mounted on the active steering actuator used to provide position feedback. The resulting active steer angle (δ_{as}) is mechanically subtracted from the driver's steer demand (δ_d) to generate a new front wheel steer angle (δ_f).

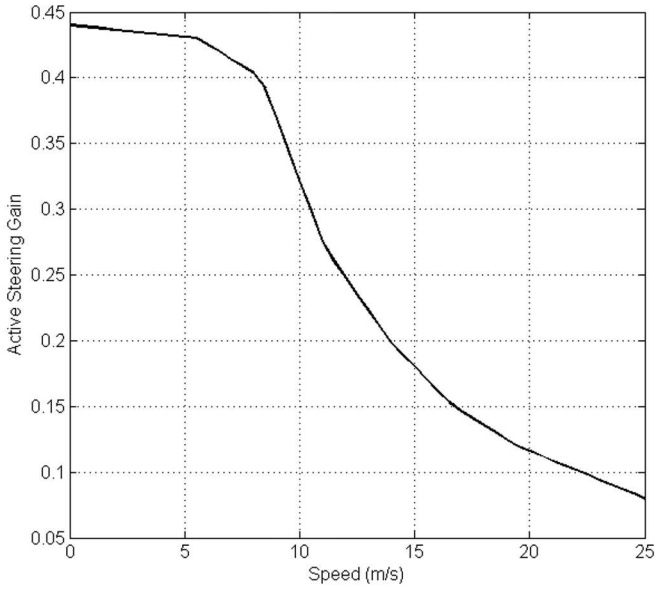

Figure 7: Active steering gain (K_δ) curve, as used in the SDTC controller [8].

Values for the active steering gain (K_δ) were obtained by Berote *et al* in [8], Figure 7. Berote used simulations of the CLEVER Vehicle's response to a ramp steer input to determine the gain value which resulted in the response/demand lateral acceleration amplitude ratio closest to 1 (or 0dB) over a range of frequencies and at a variety of speeds.

Active Steering System Performance

To ensure that the active steering system hardware was able to achieve the required dynamic response, a sine sweep test was performed. The test was performed under closed loop control (with all software filtering removed) as attempts to perform the test in open loop quickly result in the actuator drifting into its end stops. It is not safe nor practical to conduct the sine sweep with the vehicle travelling forwards at a representative speed, therefore two tests were conducted; the first with the front wheel of the CLEVER

Vehicle lifted clear of the ground (Figure 8) and the second with the wheel on the ground whilst stationary (Figure 9). The true system performance in use is expected to lie somewhere in between these two extremes. In both cases, the steering input arm (see Figure 5) was fixed in place to prevent movement.

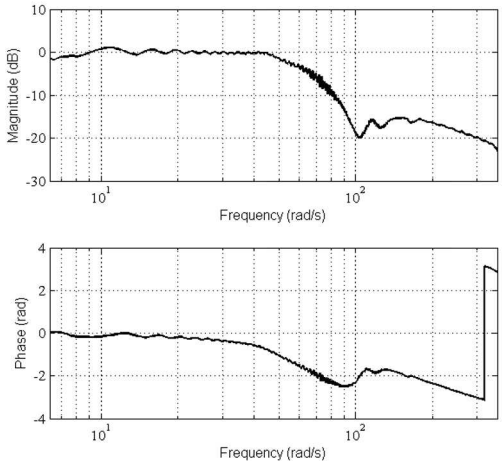

Figure 8: Active steering system response Bode plot, front wheel off ground.

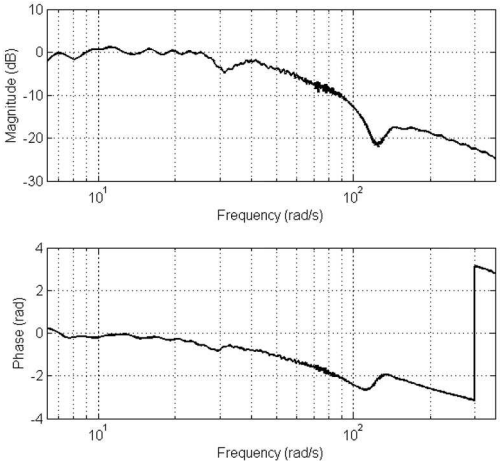

Figure 9: Active steering system Bode plot, front wheel on ground.

In the worst case scenario, with the front wheel on the ground and the vehicle stationary, the amplitude reaches the -3dB point at approximately 28.9rad/s or 4.6Hz. This is considered sufficiently higher than the human driver's bandwidth so as not to hinder the system performance. Equally, the phase lag is small up to 3Hz (18.8rad/s), indicating good performance in the anticipated operating range.

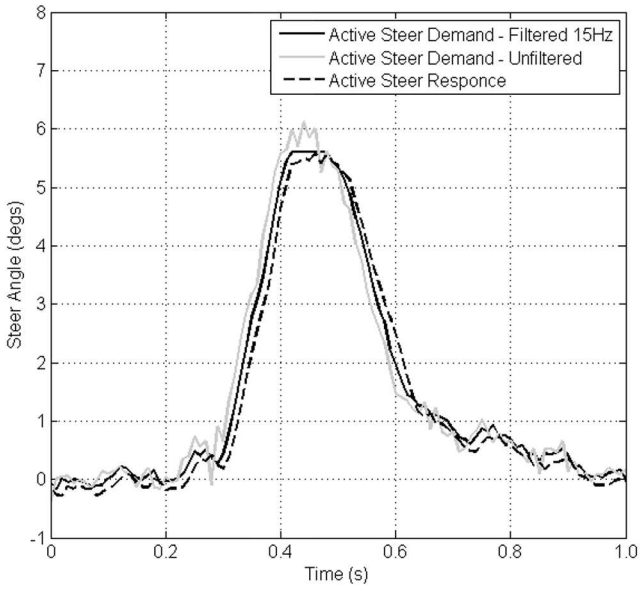

Figure 10: Active steering system demand signal (filtered and unfiltered) and the active steering system response.

Figure 10 shows the active steering system demand signal (δ_{das}) generated when a human driver applied a ramp steer input as quickly as possible whilst driving the CLEVER Vehicle at 10m/s. Also shown is the demand signal before application of the 15Hz filter and actuator stroke limits of ±5.6° (see Figure 6); finally the hydraulic active steering system's measured response is plotted. The 15Hz filter and the response characteristics of the hydraulic system contribute to a lag of approximately 0.025s. In the context of other lags associated with the vehicle's dynamics and tyre characteristics (such as the tyre relaxation length), this is not considered likely to have a significant detrimental impact on the SDTC system's performance.

4. TEST METHODOLOGY AND RESULTS

A mobile PC running software compiled using 'The MathWorks xPC Embedded Option', and fitted with a National Instruments PCI-6229 Input/Output card was used to perform both control and data logging functions. Supplementary data including GPS position and lateral acceleration was recorded using a Race Technologies DL1 data logger mounted to the rear engine module.

The CLEVER Vehicle controller logged numerous sensor and control signal channels including:

- Vehicle Speed – optical sensor on serrated front wheel brake disc.
- Drivers steer demand – contactless linear position sensor.
- Tilt angle – contactless linear position sensor.
- Active steering actuator position – Linear Variable Differential Transformer (LVDT).
- Left and right rear suspension positions – linear position sensors.
- Controller lateral acceleration estimation.
- Controller demand tilt angle and tilt angle error.
- Active steering demand angle and error.

With direct measurement not viable, where wheel loads are presented in this paper, they have been estimated using approximate suspension rate curves shown in Figure 11. The curves were generated by placing the CLEVER prototype on a set of calibrated vehicle scales, applying a roll moment to the chassis and recording both the suspension positions and the vertical wheel loads. Generating the suspension rate curves in this fashion encompasses the rear anti-roll bar's influence on the wheel loads, but excludes damping forces. Whilst attempts were made to calculate them, damping forces are omitted from the wheel load estimation as differentiation of the suspension position data, to determine the velocity, introduced unacceptable levels of error.

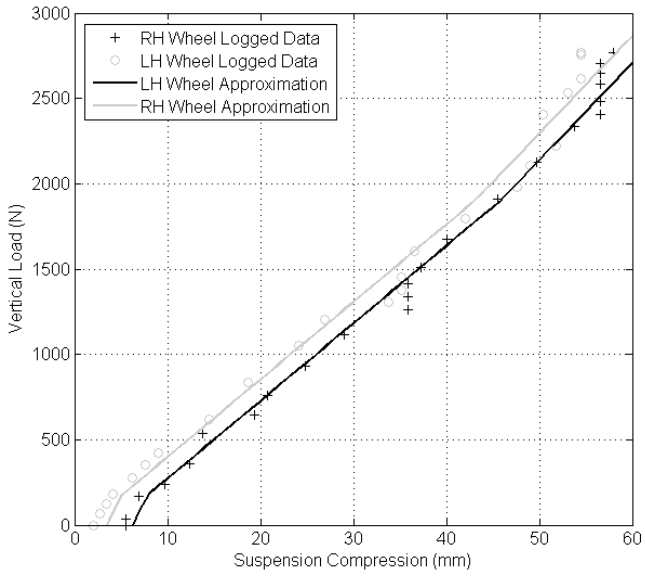

Figure 11: The 3 stage linear approximation of the CLEVER Vehicle wheel rates used to obtain estimations of the rear wheel vertical loads (F_{zl} & F_{zr}) from the suspension position data.

In order that the correct demand tilt angle (θ_d) is generated by the controller, it is important that the lateral acceleration ($\ddot{y}$) is being accurately estimated. In slowly varying conditions, comparison between the controller estimate and the measured lateral acceleration shows a good correlation despite the simplifying assumptions used in the estimate (Figure 12).

Due to packaging restrictions, the data logger used to record lateral acceleration is mounted high on the rear module of the CLEVER Vehicle, well above the roll axis. It has been established that in highly transient conditions it is subject to additional lateral accelerations resulting from the roll acceleration of the rear module; the measured lateral acceleration data therefore deviates from the controller estimate. For this reason, the controller estimate is used in this paper as the preferred lateral acceleration signal.

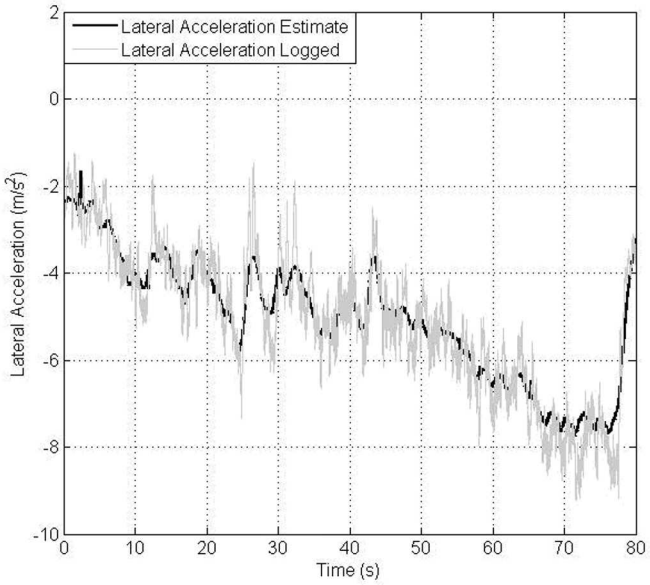

Figure 12: Lateral acceleration as estimated by the CLEVER Vehicle's controller and as measured by the data logger.

Test Scenarios

Experimental results were obtained for a series of rapid ramp steer inputs made by a human driver at three speeds between 6m/s and 10m/s in both DTC and SDTC modes. A button mounted on the CLEVER Vehicle's dashboard allowed the driver to switch between DTC and SDTC, thus facilitating back to back testing of the two modes. When in DTC mode, the active steering actuator remained under closed loop control with the demand active steering angle (δ_{das}) set to zero; in these circumstances negligible deviation from the zero demand was recorded in use.

The results presented in this paper were obtained in a single test session in a recently re-surfaced car park on the university campus; the car park surface was dry, smooth and had only a small gradient to facilitate

drainage. The same 75kg human driver was used at all times to ensure a consistent driving style and vehicle mass. The ramp steer inputs were made as quickly as possible by the driver in DTC mode, typically taking less than 0.3s to reach the demand value. The magnitude of the steer inputs was chosen to take the CLEVER Vehicle close to its roll stability limit; they were therefore smaller at higher speeds. Because of the restricted width of the test facility each steer input had to be followed, after a short dwell, by a reversal of the steer demand. The steer inputs used in the DTC case were then replicated as closely as practically possible in the SDTC case.

Inevitably, it was not possible to obtain perfectly consistent results from one test run to the next; to counter the variations in the speed and steer inputs each manoeuvre was completed multiple times. For each of the three vehicle speeds, one manoeuvre completed in DTC mode and one completed in SDTC mode were selected for comparison. The manoeuvres selected provide the best demand lateral acceleration match at each speed.

Results at 6m/s

Figures 13-20 show the test results recorded at a speed of 6m/s. A total of 51 steer input manoeuvres (31 DTC and 20 SDTC) were conducted at a nominal speed of 6m/s (Figure 13) with the resulting peak lateral accelerations ranging from 2.5 to 4m/s^2. The selected DTC and SDTC cases each show a demand lateral acceleration of approximately 3m/s^2 (Figure 14). Despite the modest size of the lateral acceleration, the CLEVER Vehicle was observed to be close to its roll moment limit during these tests with frequent lifting of the inside wheel in DTC mode.

Figure 15 shows that although no countersteering action is produced, in the SDTC case the rate at which the front wheel steer angle (δ_f) increases is reduced by the active steering system; in turn, the rate at which the lateral acceleration builds is attenuated (Figure 14). In Figure 16 the active steering angle (δ_{as}) is shown to track the demand (δ_{das}) very well, and no saturation of the active steer angle occurs. Tilt angle tracking performance is not improved in the SDTC case (Figure 17 & Figure 18) implying that the tilt actuators are not force saturated in the DTC case, and that it is the filtering of the tilt angle error (θ_e) in the controller (Figure 6) that limits the speed of the tilting response. Small reductions in the suspension position and vertical load variations (Figure 19 & Figure 20) are observed when in SDTC mode; this suggests a modest reduction in the DTC tilt actuator torque and a small improvement in vehicle stability. The effectiveness of the SDTC strategy is limited at this slow speed.

The limitations of using suspension displacement as a measure of vertical wheel load are evident in Figure 19; during testing the inside wheel was observed to lift clear of the ground in DTC mode, however the suspension was prevented from reaching full extension. Whilst the anti-roll bar's influence has been accounted for in the wheel load calculation (Figure 11), damping and friction forces mean that the minimum inside wheel load in Figure 20 is potentially exaggerated when un-laden.

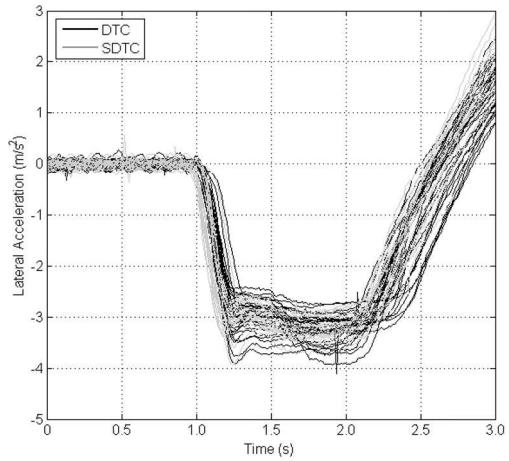

Figure 13: 6m/s - Lateral acceleration demand estimate curves for 31 steer inputs in DTC mode and 20 steer inputs in SDTC mode.

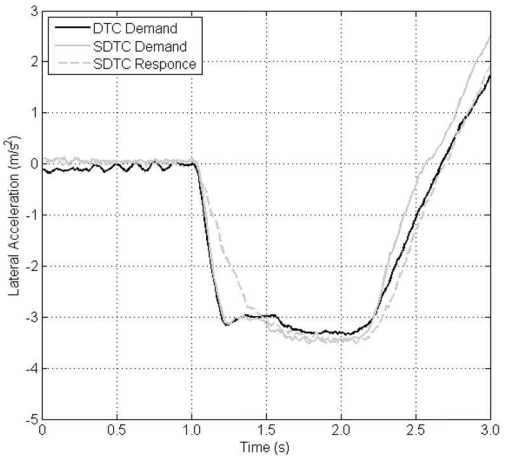

Figure 14: 6m/s - Lateral acceleration demand in the selected DTC and SDTC cases, and the resulting lateral acceleration in the SDTC case.

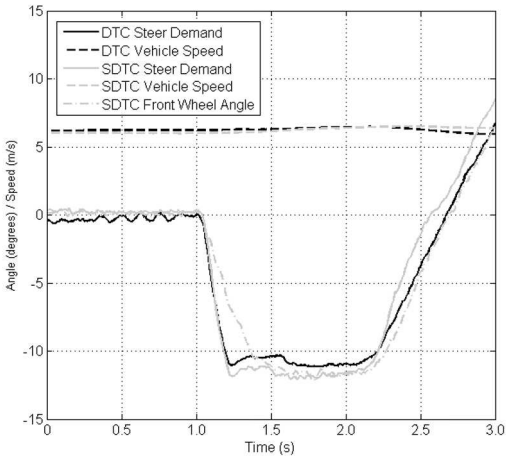

Figure 15: 6m/s - Steer demand (δ_d) and speed (U) inputs for both DTC and SDTC cases, and the resulting front wheel steer angle (δ_f) in the SDTC case.

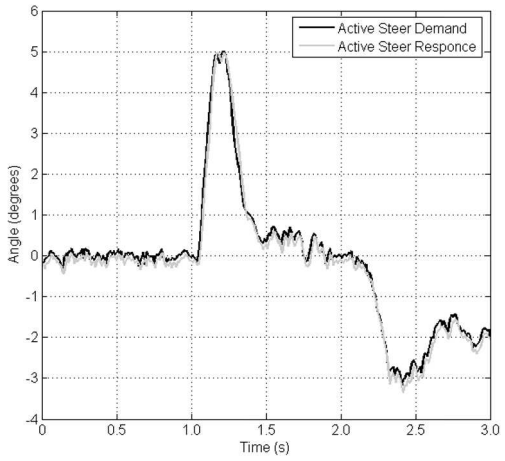

Figure 16: 6m/s - Active steer demand (δ_{das}) and response (δ_{as}) in SDTC mode.

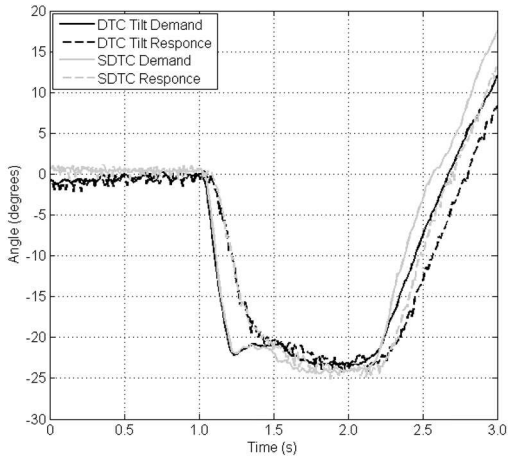

Figure 17: 6m/s - Tilt angle demand (θ_d) and response (θ) in DTC and SDTC cases.

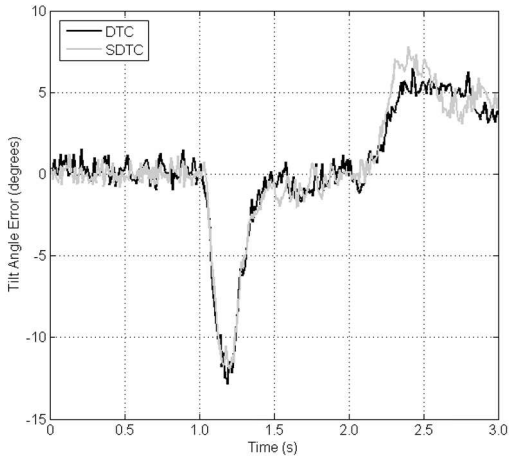

Figure 18: 6m/s - Tilt angle error (θ_e) in DTC and SDTC.

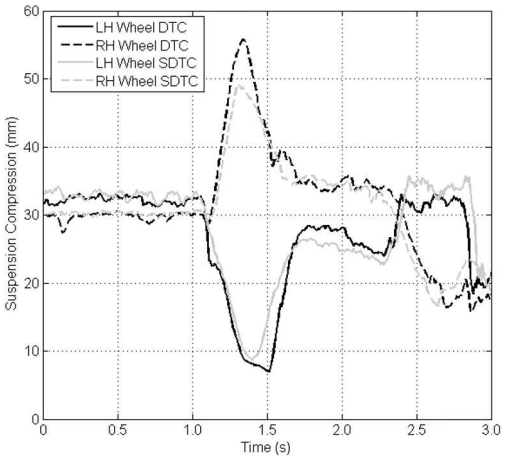

Figure 19: 6m/s - Rear suspension positions during the steer input manoeuvre.

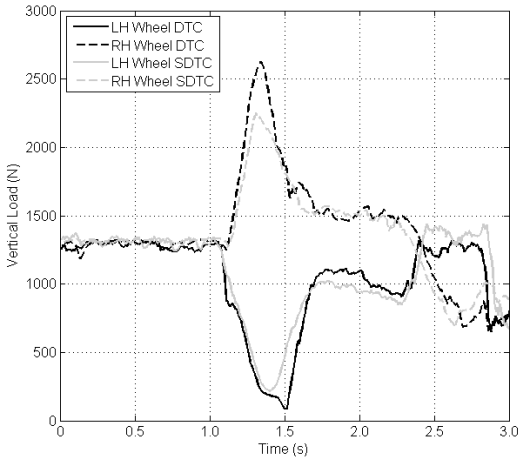

Figure 20: 6m/s - Vertical wheel loads estimated from the suspension position data.

Results at 8m/s

Figures 21-28 show the test results recorded at a speed of 8m/s. 42 steer input manoeuvres were conducted in DTC mode and 24 in SDTC mode (Figure 21) resulting in peak lateral accelerations of between approximately $3m/s^2$ and $5m/s^2$. It is noted that the driver exhibits a tendency to generate larger lateral acceleration demands in SDTC mode than DTC mode despite attempting to remain consistent; it is thought that the reduced steering torque requirement in SDTC mode is responsible. It is also noted that front wheel shimmy is evident in Figure 23; despite efforts to reduce it, some backlash remains in the steering linkages of the prototype CLEVER Vehicle which causes the wheel shimmy phenomena.

As was the case at 6m/s, no countersteering action is generated by the SDTC system in response to the selected steer input at 8m/s (Figure 23). However, in this instance, the magnitude of the steer demand (δ_d) is reduced and a larger proportion of it is attenuated momentarily by the active steering (which saturates briefly, Figure 24). The increased effectiveness of the active steering at 8m/s is also evident in the lateral acceleration curves (Figure 22), where the lateral acceleration response in SDTC mode is delayed to a greater extent than was the case at 6m/s. By delaying the onset of the lateral acceleration, the DTC actuators may apply a smaller moment between the tilting cabin and non-tilting rear module whilst achieving a similar tilting response (Figure 25).

At a forward speed of 8m/s, when operating in SDTC mode the CLEVER Vehicle shows considerably smaller variations in suspension position than occur in DTC mode (Figure 27). When comparing the minimum inside wheel vertical loads (Figure 28) to the nominal 1400N static value, a reduction in wheel load variation from 1303N to 942N is observed. This represents a 27% reduction in the load transfer in the SDTC case. Since the tilt response remains similar in both the DTC and SDTC cases (Figure 25 &

Figure 26), the reduced load transfer must result from the lower tilt moment generated by the DTC actuators, rather than from any greater balancing action of the tilted cabin mass.

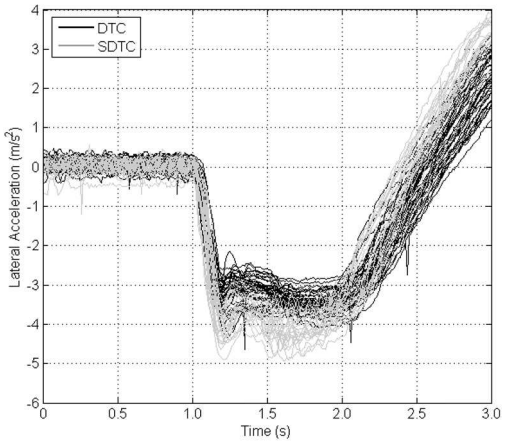

Figure 21: 8m/s - Lateral acceleration demand estimate curves for 42 steer inputs in DTC mode and 24 steer inputs in SDTC mode.

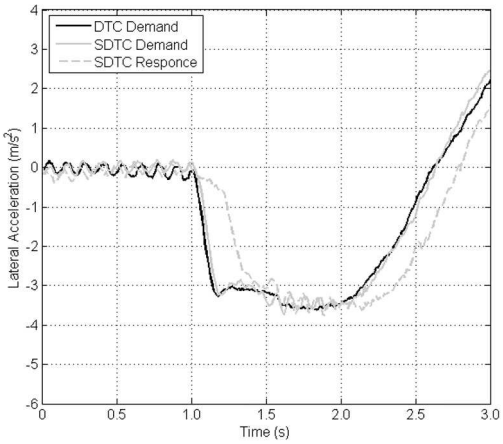

Figure 22: 8m/s - Lateral acceleration demand in the selected DTC and SDTC cases, and the resulting lateral acceleration in the SDTC case.

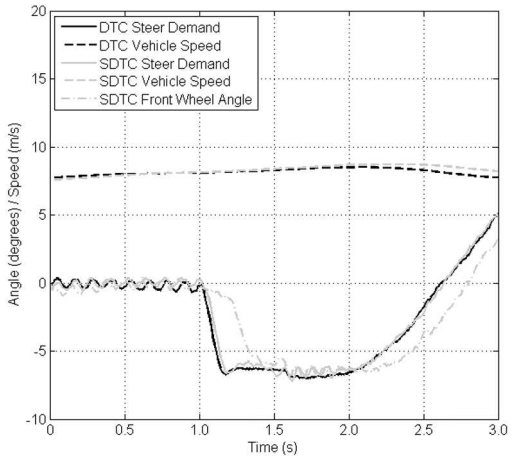

Figure 23: 8m/s - Steer demand (δ_d) and speed (U) inputs for both DTC and SDTC cases, and the resulting front wheel steer angle (δ_f) in the SDTC case.

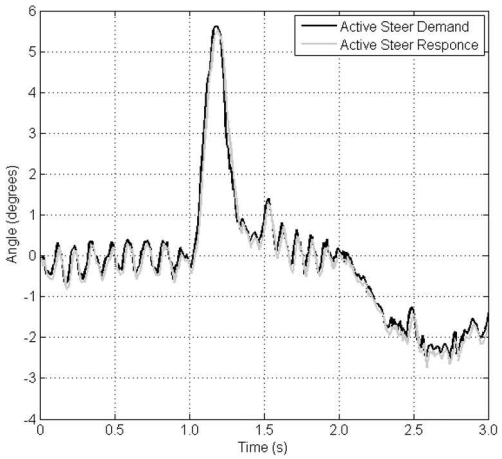

Figure 24: 8m/s - Active steer demand (δ_{das}) and response (δ_{as}) in SDTC mode.

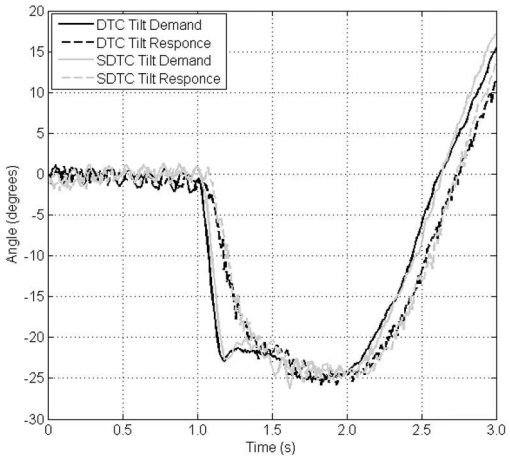

Figure 25: 8m/s - Tilt angle demand (θ_d) and response (θ) in DTC and SDTC cases.

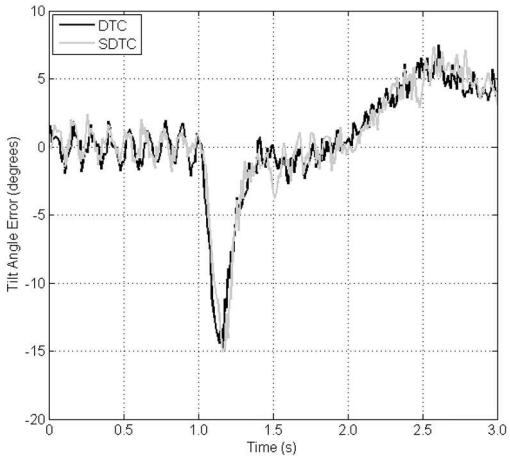

Figure 26: 8m/s - Tilt angle error (θ_e) in DTC and SDTC.

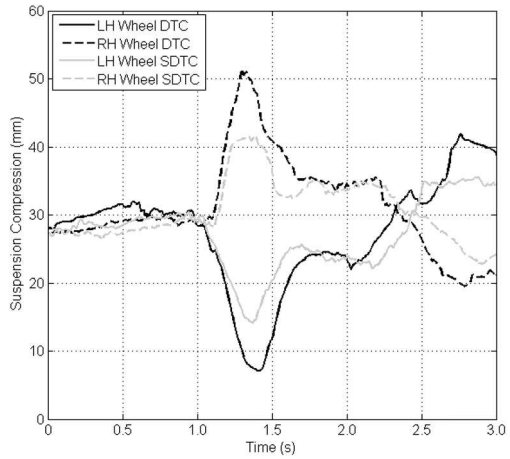

Figure 27: 8m/s - Rear suspension positions during the steer input manoeuvre.

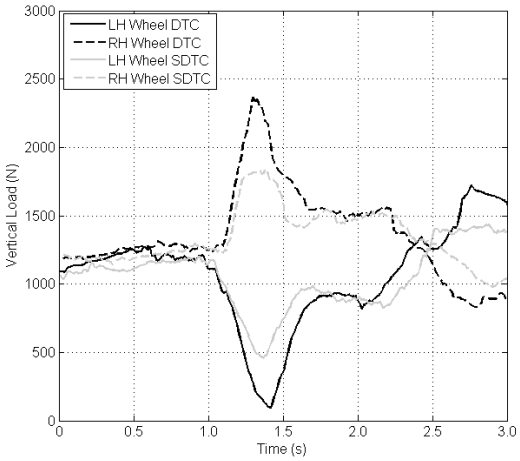

Figure 28: 8m/s - Vertical wheel loads estimated from the suspension position data.

Results at 10m/s

Figures 29-36 show the test results recorded at a speed of 10m/s. 37 steer input manoeuvres were conducted in DTC mode and 32 in SDTC mode. As was the noted at 8m/s, the lateral acceleration demand generated by the driver at 10m/s in SDTC mode is generally larger than that generated in DTC mode (Figure 29). In SDTC mode, demand lateral accelerations of up to 6m/s^2 were generated without rollover; in DTC mode the lateral acceleration demand was normally limited to approximately 4m/s^2. On two occasions the driver generated a lateral acceleration demand significantly exceeding 4m/s^2 in DTC mode which lead to his having to take corrective action as the vehicle approached roll-over. On these occasions the lateral acceleration curves can be seen to rise rapidly at t≈1.6s and t≈1.9s.

In the two cases selected for comparison, the lateral acceleration demand (Figure 30) reached a peak value of approximately 4m/s^2. The lateral acceleration response in SDTC mode was delayed by approximately 0.25s as a result of the active steering action (Figure 31). Despite the reduced active steering gain at 10m/s (Figure 7), the active steering angle (δ_{as}) is seen to saturate (Figure 32). The higher vehicle speed results in a larger tilt angle demand (θ_d) and consequently an increased tilt angle error (θ_e) (Figure 34). Once again, the tilting response was similar in both DTC and SDTC modes (Figure 33).

Figure 35 and Figure 36 show a significant reduction in the suspension position and wheel load variations that occur during the ramp steer manoeuvre when in SDTC mode. In this mode the inside wheel experiences a minimum load of 560N, during the same manoeuvre conducted in DTC mode the minimum load is 79N. If the wheel load variations from the nominal static load of 1400N are considered, the 840N variation in SDTC mode represents a 36% reduction from the 1321N variation that occurs in DTC mode. Again, the influence of friction and damping is thought to mask the full extent of the inside wheel load variations, particularly at the very low loads recorded in the DTC case.

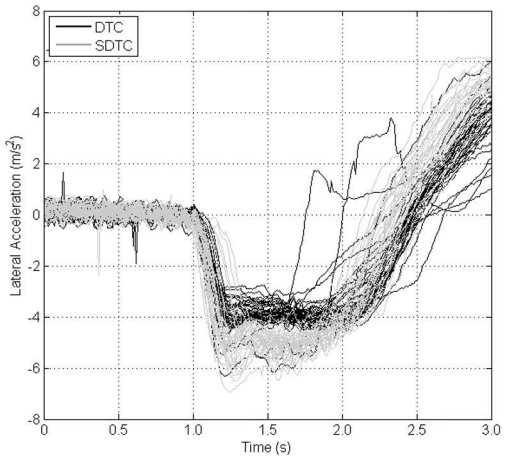

Figure 29: 10m/s - Lateral acceleration demand estimate curves for 37 steer inputs in DTC mode and 32 inputs in SDTC mode.

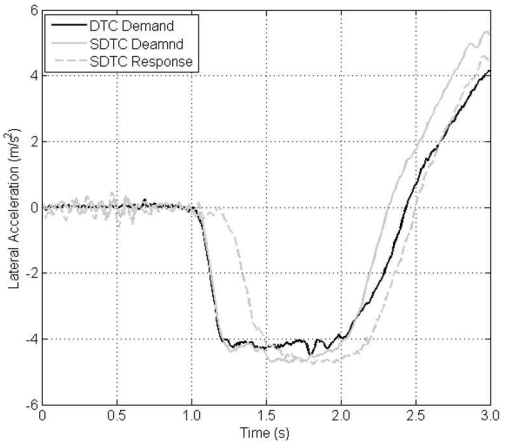

Figure 30: 10m/s - Lateral acceleration demand in the selected DTC and SDTC cases, and the resulting lateral acceleration in the SDTC case.

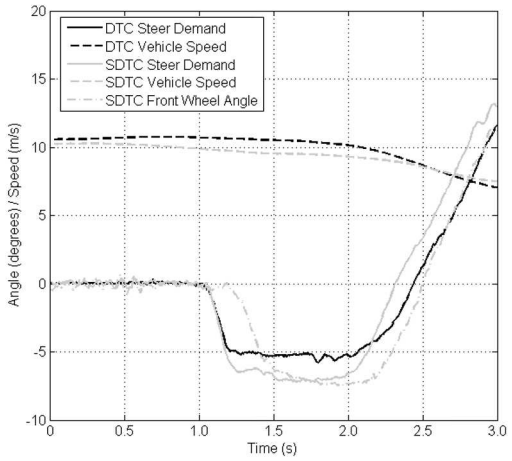

Figure 31: 10m/s - Steer demand (δ_d) and speed (U) inputs for both DTC and SDTC cases, and the resulting front wheel steer angle (δ_f) in the SDTC case.

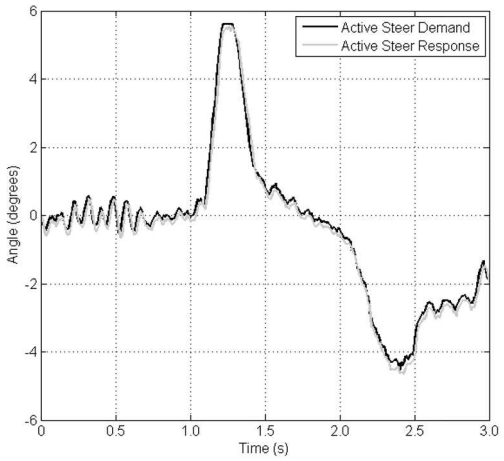

Figure 32: 10m/s - Active steer demand (δ_{das}) and response (δ_{as}) in SDTC mode.

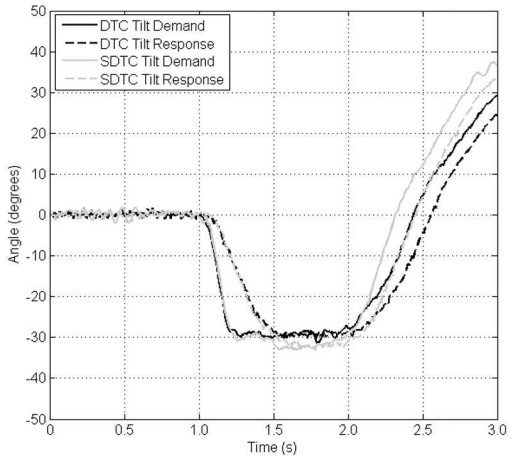

Figure 33: 10m/s - Tilt angle demand (θ_d) and response (θ) in DTC and SDTC cases.

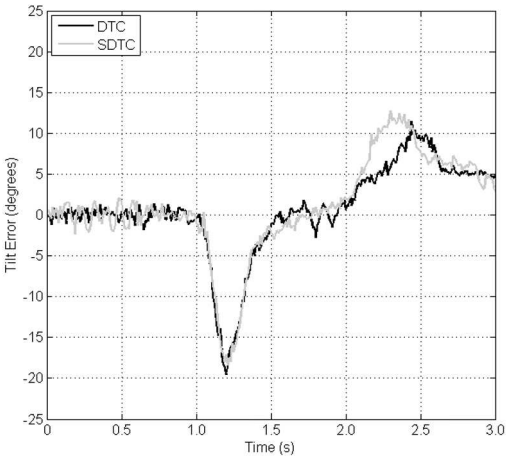

Figure 34: 10m/s - Tilt angle error (θ_e) in DTC and SDTC.

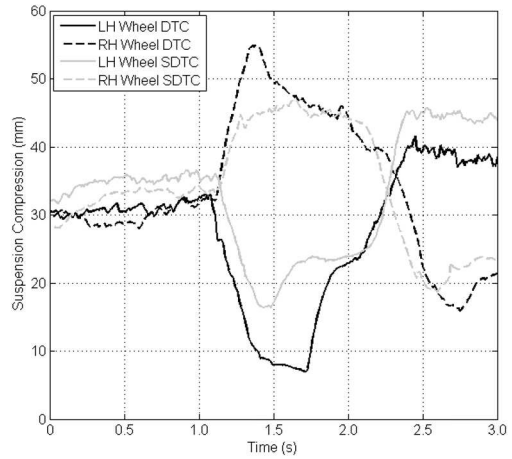

Figure 35: 10m/s - Rear suspension positions during the steer input manoeuvre.

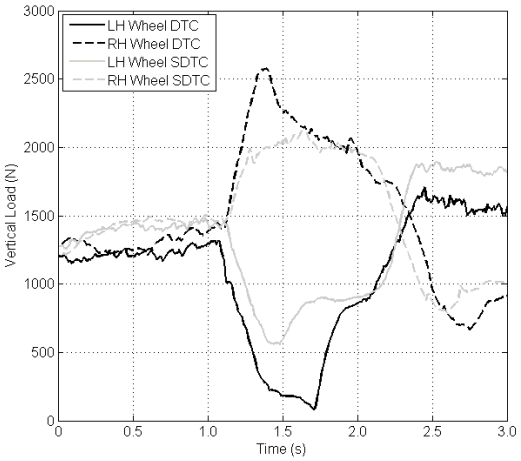

Figure 36: 10m/s - Vertical wheel loads estimated from the suspension position data.

Subjective Observations

During testing of the CLEVER Vehicle, a number of subjective observations were made by the driver.

Firstly; in SDTC mode the steering torque requirement (or steering weight) is reduced considerably; this is thought to be the result of the active steering acting to 'absorb' the driver's steer input. This trait was considered a positive one by the driver as it reduced the physical effort required to pilot the CLEVER Vehicle. It was also noted that the driver did not feel significant levels of 'kickback' through the steering wheel from the 'in-series' active steering system, perhaps helped by the use of a worm type reduction steering box.

Despite the data showing no appreciable difference in tilt response, in SDTC mode the driver's perception was that the vehicle responded more quickly than it did in DTC mode. This may be due to a reduction in the rear module roll rate, and the associated increase in the true tilt angle rate that results. It may also result from the reduced steering torque requirement (described above) allowing larger, faster steer inputs to be made.

Delays in generating lateral acceleration, introduced by the active steering system in SDTC mode, felt like mild understeer. This is considered an acceptable characteristic as most drivers are familiar with a vehicle which understeers and the short duration of the sensation did not notably inhibit the driver's ability to control the vehicle's heading.

5. CONCLUSIONS

This paper builds upon earlier simulation-based research conducted at the University of Bath and provides experimental results showing the effectiveness of a combined Steering Direct Tilt Control

system in improving Narrow Tilting Vehicle stability during highly transient manoeuvres. Comparative ramp steer input tests were performed in a prototype vehicle, using both Direct Tilt Control and Steering Direct Tilt Control strategies, at three different speeds. Suspension position data was used to estimate the vertical loads supported by each of the two rear wheels and therefore quantify the vehicle's roll stability.

The effectiveness of the SDTC system was shown to vary as a function of speed; at lower speeds it was shown to perform in a similar manner to a DTC system. However, small increases in the vehicle's forward speed yielded significant reductions in the wheel load variation experienced in SDTC mode. At 10m/s the wheel load variation in SDTC mode was 36% lower than that recorded in DTC mode, significantly enhancing the vehicle's stability.

Finally, it was judged that the driving characteristics of a Narrow Tilting Vehicle were not unacceptably compromised, and in some ways were enhanced, by the use of a Steering Direct Tilt Control system.

FUNDING

This work was supported by an Engineering and Physical Sciences Research Council (EPSRC) studentship.

DECLARATION OF CONFLICTING INTERESTS

The authors declare than there is no conflict of interest.

LIST OF CAPTIONS

Figure 1: The CLEVER Vehicle complete with bodywork.

Figure 2: CLEVER Vehicle prototype demonstrating its lack of roll stability in transient conditions.

Figure 3: CLEVER Vehicle kinematic parameters with rear module constrained in yaw.

Figure 4: Steady state moment reserve shown with the cabin both tilting and fixed upright.

Figure 5: In-series active steering actuator installation.

Figure 6: SDTC system block diagram.

Figure 7: Active steering gain (K_δ) curve, as used in the SDTC controller [8].

Figure 8: Active steering system response Bode plot, front wheel off ground.

Figure 9: Active steering system Bode plot, front wheel on ground.

Figure 10: Active steering system demand signal (filtered and unfiltered) and the active steering system response.

Figure 11: The 3 stage linear approximation of the CLEVER Vehicle wheel rates used to obtain estimations of the rear wheel vertical loads (F_{zl} & F_{zr}) from the suspension position data.

Figure 12: Lateral acceleration as estimated by the CLEVER Vehicle's controller and as measured by the data logger.

Figure 13: 6m/s - Lateral acceleration demand estimate curves for 31 steer inputs in DTC mode and 20 steer inputs in SDTC mode.

Figure 14: 6m/s - Lateral acceleration demand in the selected DTC and SDTC cases, and the resulting lateral acceleration in the SDTC case.

Figure 15: 6m/s - Steer demand (δ_d) and speed (U) inputs for both DTC and SDTC cases, and the resulting front wheel steer angle (δ_f) in the SDTC case.

Figure 16: 6m/s - Active steer demand (δ_{das}) and response (δ_{as}) in SDTC mode.

Figure 17: 6m/s - Tilt angle demand (θ_d) and response (θ) in DTC and SDTC cases.

Figure 18: 6m/s - Tilt angle error (θ_e) in DTC and SDTC.

Figure 19: 6m/s - Rear suspension positions during the steer input manoeuvre.

Figure 20: 6m/s - Vertical wheel loads estimated from the suspension position data.

Figure 21: 8m/s - Lateral acceleration demand estimate curves for 42 steer inputs in DTC mode and 24 steer inputs in SDTC mode.

Figure 22: 8m/s - Lateral acceleration demand in the selected DTC and SDTC cases, and the resulting lateral acceleration in the SDTC case.

Figure 23: 8m/s - Steer demand (δ_d) and speed (U) inputs for both DTC and SDTC cases, and the resulting front wheel steer angle (δ_f) in the SDTC case.

Figure 24: 8m/s - Active steer demand (δ_{das}) and response (δ_{as}) in SDTC mode.

Figure 25: 8m/s - Tilt angle demand (θ_d) and response (θ) in DTC and SDTC cases.

Figure 26: 8m/s - Tilt angle error (θ_e) in DTC and SDTC.

Figure 27: 8m/s - Rear suspension positions during the steer input manoeuvre.

Figure 28: 8m/s - Vertical wheel loads estimated from the suspension position data.

Figure 29: 10m/s - Lateral acceleration demand estimate curves for 37 steer inputs in DTC mode and 32 inputs in SDTC mode.

Figure 30: 10m/s - Lateral acceleration demand in the selected DTC and SDTC cases, and the resulting lateral acceleration in the SDTC case.

Figure 31: 10m/s - Steer demand (δ_d) and speed (U) inputs for both DTC and SDTC cases, and the resulting front wheel steer angle (δ_f) in the SDTC case.

Figure 32: 10m/s - Active steer demand (δ_{das}) and response (δ_{as}) in SDTC mode.

Figure 33: 10m/s - Tilt angle demand (θ_d) and response (θ) in DTC and SDTC cases.

Figure 34: 10m/s - Tilt angle error (θ_e) in DTC and SDTC.

Figure 35: 10m/s - Rear suspension positions during the steer input manoeuvre.

Figure 36: 10m/s - Vertical wheel loads estimated from the suspension position data.

APPENDIX

Notation	Description
a_c	Longitudinal position of cabin mass from front axle
F_{zf}	Vertical load supported by front wheel at rest
F_{zl}	Vertical load supported by left rear wheel at rest with cabin upright
F_{zr}	Vertical load supported by right rear wheel at rest with cabin upright
g	Acceleration due to gravity
h_c	Height of cabin mass CG from ground plane in upright position
h_r	Height of rear module mass CG from ground plane
h_{tb}	Height of tilt bearing from ground plane
K_δ	Active steering gain
L	Wheelbase length
l_c	Longitudinal position of tilt bearing from front axle
m	Total vehicle mass
M_c	Moment capacity (roll)
m_c	Cabin mass (including driver and un-sprung mass)
M_r	Moment reserve (roll)

m_r	Rear engine module mass (including un-sprung mass)
r	Corner radius
r_t	Radius of tyre cross section
T	Track width
U	Vehicle forward speed
$\ddot{y}$	Lateral acceleration
y_c	Lateral displacement of cabin CG
y_f	Lateral displacement of tyre contact patch
Z_c	Height of cabin mass CG from ground plane (dynamic)
δ_{as}	Active steer angle (actual)
δ_d	Steer demand angle
δ_{das}	Active steer demand angle
δ_e	Active steer angle error
δ_f	Front wheel steer angle (actual)
δ_r	Rear wheel steer angle
θ	Tilt angle (actual)
θ_d	Tilt angle demand
θ_e	Tilt angle error
ξ	Tilt axis inclination from horizontal plane

REFERENCES

[1] Hollmotz, L., Sohr, S., Johannsen, H., 2005. CLEVER – A Three Wheel Vehicle With a Passive Safety Comparable to Conventional Cars. *Proceedings of the 19th International Technical Conference on the Enhanced Safety of Vehicles*, June 6-9, 2005, Washington, D.C., USA.

[2] Chiou, J.C., Chen, C.L., 2008. Modeling and Verification of a Diamond-Shape Narrow-Tilting-Vehicle. *IEEE Transactions on Mechatronic*, 13(6), pp.978-691.

[3] Karnopp, D., Fang, C., 1992. A Simple Model of Steering Controlled Banking Vehicles. *ASME Dynamic Systems and Control (Transportation Systems),* 44, pp.15-28.

[4] Drew, B., Edge, K., Barker, M., Darling, J., Owen, G., 2005. System Development for Hydraulic Tilt Actuation of a Tilting Narrow Vehicle. *9th Scandinavian International Conference on Fluid Power, SICFP '05*, June 1-3, 2005, Linköping, Sweden.

[5] Snell, S.A., 1998. An Active Roll Moment Control Strategy for Narrow Tilting Commuter Vehicles. *Vehicle System Dynamics*, 29(5), pp.277-307.

[6] Kidane, S., Rajamani, R., Alexander, L., Starr, P., Donath, M., 2009. Development and Experimental Evaluation of a Tilt Stability Control System for Narrow Commuter Vehicles. *IEEE Transactions on Control Systems Technology,* 18(6), pp.1266-1279.

[7] So, S.G., Karnopp, D., 1997. Switching Strategies for Narrow Ground Vehicles with Dual Mode Automatic Tilt Control. *International Journal of Vehicle Design*, 18(5), pp.518-532.

[8] Berote, J., Darling, J., Plummer, A.R., 2011. Development of a Tilt Control Method for a Narrow Track Three Wheeled Vehicle. *Proceedings of the Institution of Mechanical Engineers, Part D, Journal of Automobile Engineering,* 226(1), pp.48-69.

[9] Kidane, S., Rajamani, R., Alexander, L., Starr, P., Donath, M., 2007. Experimental Investigation of a Narrow Leaning Vehicle Tilt Control System. *Proceedings of the 2007 American Control Conference*, July 11-13, New York City, USA.

[10] Furuichi, H., Huang, J., Matsuno, T., Fukuda, T., 2012. Dynamic Modelling of Three Wheeled Narrow Tilting Vehicle and Corresponding Experiment Verification. *IEEE/RSJ International Conference on Intelligent Robots and Systems*, 07/12/12, Vilamoura, Portugal.

[11] Furuichi, H., Huang, J., Matsuno, T., Fukuda, T., 2012. Dynamic Modeling of Three Wheeled Narrow Tilting Vehicle and Optimal Tilt Controller Design. *IEEE International Symposium on Micro-NanoMechatronics and Human Science (MHS) 2012*. 04/11/12-07/11/12, Nagoya, Japan.

[12] Barker, M., 2006, *Chassis Design and Dynamics of a Tilting Three-Wheeled Vehicle*. Thesis (Ph.D.). University of Bath, Bath, United Kingdom.

[13] Berote, J.J.H., 2010. *Dynamics and Control of a Tilting Three Wheeled Vehicle*. Thesis (Ph.D.). University of Bath, Bath, United Kingdom.

[14] Barker, M., Drew, B., Darling, J., Edge, K.A., Owen, G.W., 2009. Steady-State Steering of a Tilting Three-Wheeled Vehicle. *Vehicle System Dynamics*, 48(7), pp.815-830.

[15] Drew, B., 2007. *Development of Active Tilt Control for a Three-Wheeled Vehicle*. Thesis (Ph.D.). University of Bath, Bath, United Kingdom.